Available online at www.sciencedirect.com
SCIENCE DIRECT
Catalysis Today 102–103 (2005) 254–258
CATALYSIS TODAY
www.elsevier.com/locate/cattod

Rh/GNF catalysts: Characterization and catalytic performance in methylcyclopentane reactions

Z. Paál [a,*], D. Teschner [a,d], N.M. Rodriguez [b], R.T.K. Baker [b], L. Tóth [c], U. Wild [d], R. Schlögl [d]

[a] *Institute of Isotopes, CRC, Hungarian Academy of Sciences, P.O. Box 77, Budapest H-1525, Hungary*
[b] *Catalytic Materials LLC, 1750 Washington St., Holliston, MA 01746, USA*
[c] *Institute of Technical Physics and Materials Science, Hungarian Academy of Sciences, P.O. Box 49, Budapest H-1525, Hungary*
[d] *Fritz-Haber-Institut der MPG, Faradayweg 4-6, D-14195 Berlin, Germany*

Available online 24 March 2005

Abstract

Rh catalysts supported on two graphite nanofiber structures (herring-bone – GNF-H and platelet – GNF-P) have been synthesized and characterized by XPS and HRTEM. Rh was partly oxidized after storage in air but reduced to Rh by H_2 treatments at 473 K. The graphitic character of GNF-P was closer to that of highly ordered pyrolytic graphite than that of GNF-H. H_2 treatment hardly affected the properties of the graphite component. HRTEM shows the appropriate graphite structures and Rh crystallites, mainly on the surface of GNF. The catalytic properties in ring opening of methylcyclopentane (MCP) were close to each other, Rh/GNF-P with more ordered graphite structure favoring ''ring opening'' to C_6 alkanes. The ring opening reaction was ''selective'', producing more methylpentanes than hexane. This selectivity increased at higher H_2 pressures. As reported earlier, 2-methylpentane was the main source of $<C_6$ fragments. Considerably less fragments were produced on both Rh/GNF samples than on other Rh catalysts, due, likely, to more surface H on metallic active sites supplied from hydrogen stored by the GNF supports.

Keywords: Rh; Graphite nanofiber; Methylcyclopentane ring opening; XPS; Electron microscopy

1. Introduction

Graphite nanofibers (GNF) are promising new supports for metal catalysts [1]. Their graphitic platelets can be present in three different geometrical arrangements: ''platelet'', ''ribbon'' and ''herring-bone'' [2]. The excellence of Pt/GNF catalysts in hexane isomerization was attributed to their hydrogen storage ability [3]. Pt/GNF catalysts favored reactions requiring hydrogen, such as alkane isomerization [4]. Their XPS study indicated a carbon structure close but not quite identical to that of highly ordered pyrolytic graphite (HOPG), the structure of GNF-H being farthest from HOPG [4]. In addition to Pt, a few other metals, including Rh on GNF support have been tested in catalytic reactions, like hydroformylation [5] and C=C bond hydrogenation [6].

The present study will describe two Rh/GNF catalysts. They were characterized with XPS and HRTEM. Their catalytic performance was tested in the ring opening of methylcyclopentane (MCP). The main reaction of MCP is the splitting of the ring to give C_6 alkanes [7,8]. Rhodium is much more active in the rupture of C–C bonds than Pt, producing $<C_6$ fragments with higher selectivities [9]. Nevertheless, Rh is also able to split just one C–C bond of MCP (like Pt) and can produce hexane isomers as main products [10]. The presence or absence of support or its nature plays a minor role in determining the relative abundance of ring opening products (ROP, i.e. C_6 alkanes) or $<C_6$ fragments. Although splitting of the MCP ring involves also hydrogenolytic C–C bond rupturing, the term ''ring opening'' is justified by the rigid geometry of the five-membered ring, involving, very likely a less dissociated

* Corresponding author. Tel.: +36 1 392 2531; fax: +36 1 392 2533.
E-mail address: paal@iserv.iki.kfki.hu (Z. Paál).

0920-5861/$ – see front matter © 2005 Elsevier B.V. All rights reserved.
doi:10.1016/j.cattod.2005.02.024

(likely flat-lying) surface intermediate [8,11], different from that leading to alkane hydrogenolysis [12].

2. Experimental

The preparation of the GNF supports involved heating a mixture of C_2H_4/H_2 in the presence of metal catalysts: a Fe based catalyst for platelet-type (GNF-P) and Cu–Ni for the herring-bone type (GNF-H) [12]. The Rh/GNF catalysts were prepared by impregnating these supports with Rh salts [5]. $RhCl_3$ dissolved in ethanol was used for Rh/GNF-H and the solution of Rh nitrate in butanol for GNF-P. Drying (323–343 K), calcination (523 K) and reduction between 473 and 673 K followed.

XPS analysis of the samples was carried out using a Leybold LHS 12 MCD instrument [9,14]. Mg Kα excitation was used (pass energy, PE = 48 eV). The peaks were evaluated after satellite subtraction applying a Shirley background, using literature sensitivity factors for quantitative analysis [15].

A JEOL 3010 high-resolution electron microscope (HRTEM) was used to analyze individual metallic particles [16]. Their size distribution was determined from electron micrographs of lower magnification taken by a JEOL 200 FXII instrument [13].

Catalytic reactions used 10 Torr MCP and 120–480 Torr H_2, between 468 and 513 K in a closed loop reactor. The products were analyzed by capillary GC [11,17].

3. Results and discussion

3.1. Electron microscopy

The average metal particle sizes were 2.9 ± 1.3 nm (for 5% Rh/GNF-P) and 3.8 ± 1.7 nm (for 4% Rh/GNF-H). The structure of the GNF support is clearly distinguished on the HRTEM pictures. Rather well-structured Rh particles are observed, mainly on the surface of the GNF supports (Figs. 1 and 2). They can be slightly embedded into graphite. Various lattice spacings appeared on different grains: Fourier-transform analysis identified Rh[1 1 0] lattice image on both Rh/GNF samples. Most of the crystals have cubo-octahedral shapes and exhibit typically angular structure, surrounded by planar crystal faces. In some cases aggregates of two to three particles could also be observed.

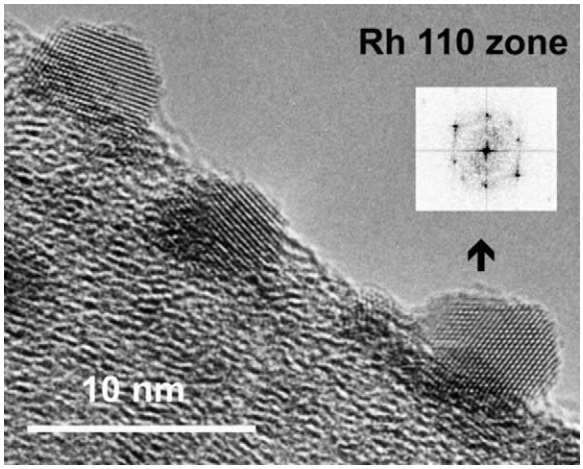

Fig. 2. High-resolution electron micrograph of the ‘‘as prepared’’ Rh/GNF-H sample with Rh nanoparticles on the GNF matrix. The insert shows Fourier transform analysis of the Rh particle indicated by the arrow, showing nearly perfect {1 1 0} orientation.

3.2. Electron spectroscopy

The surface composition measured by XPS is seen in Table 1. One of the samples: GNF-P contained Fe and Cl impurity, ca. 0.5% each. Fe remained from the iron catalyst used for GNF preparation; its removal with diluted HCl was,

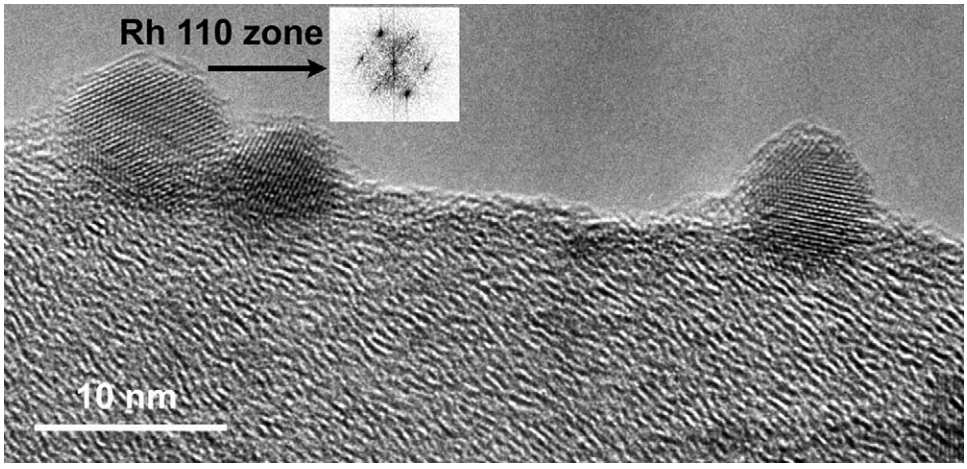

Fig. 1. High-resolution electron micrograph of the ‘‘as prepared’’ Rh/GNF-P sample with Rh nanoparticles on the GNF matrix. The insert shows Fourier transform analysis of the Rh grain at far left, close to {1 1 0} orientation. The somewhat blurred three parallel lines (from to right to bottom left) indicate the presence of more than one particle behind each other.

Table 1
Composition (at.%) of the two Rh/GNF catalysts determined by XPS

Component	"As is"	H_2, 300 K	H_2, 473 K
(a) Catalyst: 4% Rh/GNF-H			
C 1s	93.2	94.1	94.9
Rh3d	2.1	2.3	2.6
O 1s	4.7	3.6	2.5
(b) Catalyst: 5% Rh/GNF-P[a]			
C 1s	91.5	92.9	94.7
Rh3d	3.4	3.7	3.6
O 1s	5.1	3.4	1.7

[a] Containing ~0.5% Fe and ~0.5% Cl, their amount being almost independent of the treatment. The compositions given have been obtained after normalizing C + Rh + O = 100%.

accordingly, not complete and even chlorine was retained. The shape of the C 1s peak was close to that of highly ordered pyrolytic graphite (HOPG) with clearly distinguished plasmon loss peak. The structure of the graphite was less perfect in GNF-H, as reported also earlier [4,13]: the full-width-at-half-maximum (fwhm) value for HOPG was measured to be 0.9 eV [4]. The fwhm values were between 1.23 and 1.27 eV for Rh/GNF-H and 1–1.03 eV for Rh/GNF-P after various treatments. The asymmetric difference spectra [Rh/GNF-H—HOPG] in Fig. 3 indicate a line broadening plus a minor BE maximum shift of the C 1s peak. One difference spectrum [Rh/GNF-P minus HOPG] is also shown: this is less asymmetric, as expected when both line broadening and BE(max) shift were less pronounced.

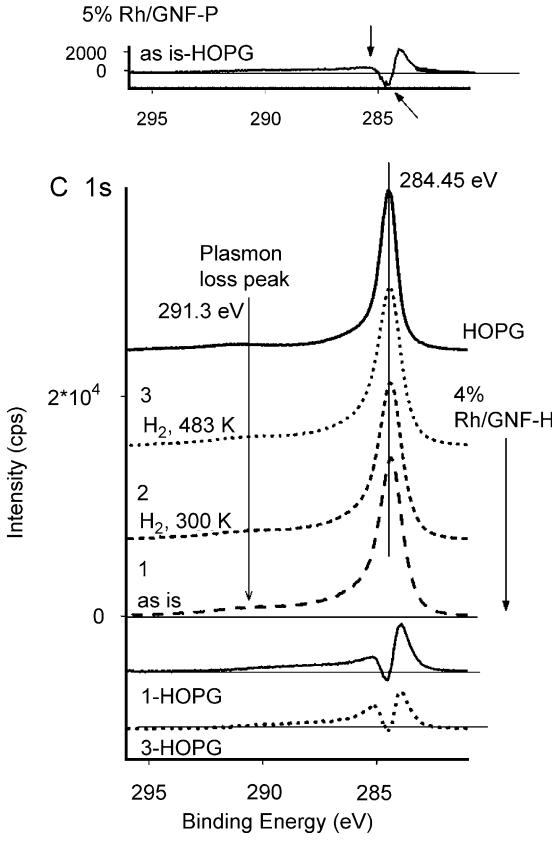

Fig. 3. XPS of C 1s peaks of HOPG and GNF-H in three different states, two difference spectra [GNF-H—HOPG] are also shown: in the "as is" state and after H_2 at 483 K. An analogous difference spectrum ["as is"—HOPG] is seen on the top inset, adjusted to the same intensity scale. Arrows show its shape differences from those of [Rh/GNF-H—HOPG].

Rh and Rh_2O_3 were simultaneously present in the "as is" samples. Fig. 4a shows them in nearly equal amounts in GNF-H. Some Rh oxide remained after H_2 treatment at room temperature. H_2 at 483 K completed the reduction, like that reported for Rh black [9]. The shape of the Rh 3d peaks in Rh/GNF-P and Rh/GNF/H were very similar after analogous treatments.

The O content of a GNF sample could reportedly reach ~7% [18]. "Several unresolved peaks between 529.9 and 532 eV" in the O 1s line were reported for oxygen detected on high-surface carbons [19]. Components with BE values up to ~534 eV appeared in Pt/GNF samples [4]. Two oxygen species – identified earlier [20] as >C–O– (533.0 ± 0.3 eV) and >C=O (531.4 ± 0.3 eV) structures – were the main components in the O 1s line (Fig. 4b). The higher oxygen content of Rh/GNF samples (up to 5% as opposed to ~3% on Pt/GNF catalysts) can partly be due to the presence of Rh_2O_3 compound and even the Fe impurity of Rh/GNF-P could be partly oxidized. That is why H_2 treatment decreased here more strongly the O percentage than with Pt/GNF where just chemisorbed O was present on Pt [4]. Reduction removed first the lower BE components (BE

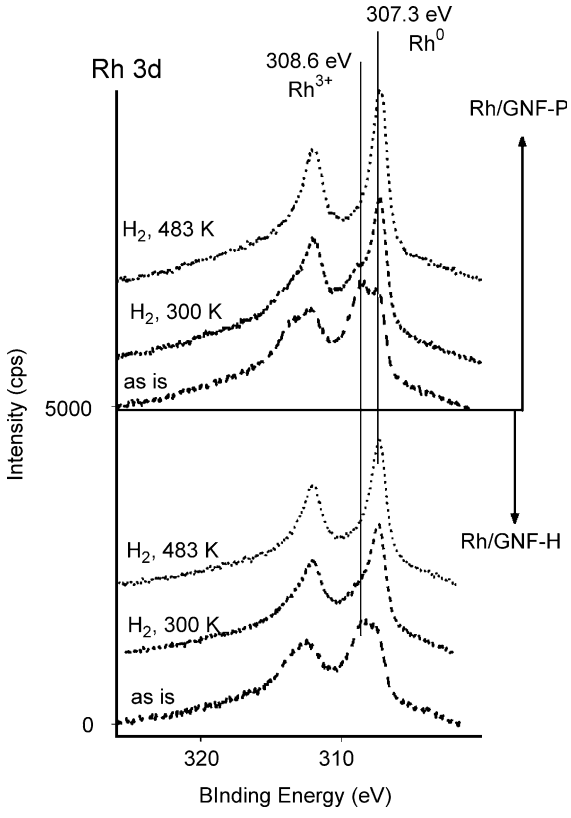

Fig. 4. Spectra of Rh/GNF-H after different treatments: (a) lower panel: Rh 3d; (b) upper panel: relative intensities of O 1s, normalized to the corresponding C 1s intensities.

~530 eV, i.e., metal oxides). H_2 at 483 K affected the C=O bonds, too. Single C–O– structures were most stable [21].

3.3. Catalytic tests

In the view of literature results [9–11,17], not very dramatic differences can be expected between the behavior of various Rh samples, since this metal has a strong activity in breaking C–C bonds. The *activity* of the two Rh/GNF catalysts is compared in Fig. 5. Two major classes of products were produced from MCP: ring opening products (ROP), i.e., 2-methylpentane (2MP), 3-methylpentane (3MP) and hexane (nH) as well as $<C_6$ fragments. The overall rate showed a strong positive hydrogen order but the relative preference of the products was widely influenced by the reaction conditions. Higher $p(H_2)$ increased the yields of the main products: C_6 alkanes from ring opening. The yields of fragments were almost constant (Fig. 5). Rh/GNF-H showed higher fragmentation activity (to $<C_6$) at intermediate hydrogen pressure. Its activity to ROP was less promoted by high $p(H_2)$ than that of Rh/GNF-P. The higher activity of Rh/GNF-P in nondegradative reactions is obvious.

Table 2 compares the selectivity of fragmentation and its depth (the ζ value, i.e., the number of fragments per feed molecule fragmented) was the lowest with Rh/GNF catalysts as compared to others (Rh black, Rh on alumina, silica or ceria). This can be attributed to the highest surface hydrogen concentration on Rh/GNF catalysts, due to the hydrogen storage capacity of that support. Reverse spillover supplied H to the metallic sites. One cannot expect more dramatic differences between the catalytic properties of Rh catalysts of different preparation [17,22–24]: the large difference (46% versus 3.5–5%) between the fragmentation selectivities is significant, considering the general behavior of Rh. More fragments were produced at higher temperature and at lower $p(H_2)$. Here the values of ζ were lowest on Rh/GNF catalysts. All these demonstrate the advantage of Rh/GNF samples in nondegradative reaction versus oxide-supported catalysts, even with similar dispersion.

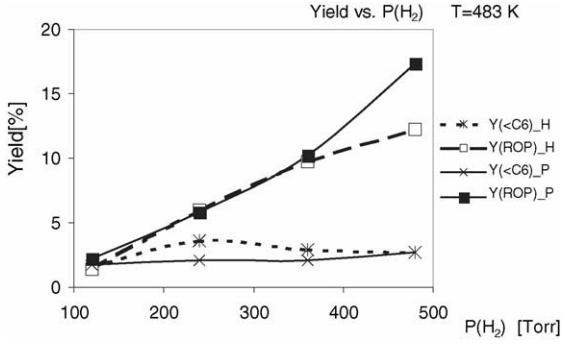

Fig. 5. Yields of ring opening products (ROP) and fragments as a function of the hydrogen pressure, $p(H_2)$, p(MCP) = 10 Torr, reaction temperature, T = 483 K.

Table 2
Fragment selectivity and ζ "fragmentation factor"[a] on different Rh catalysts

Catalyst	Disp. (%)	468 K, $p(H_2)$ = 480 Torr		513 K, $p(H_2)$ = 120 Torr		Reference
		S(<C_6)	ζ	S(<C_6)	ζ	
Rh black	2	46[b]	2.55[b]	59	3.7[c]	[9]
3% Rh/Al_2O_3[b]	25	18	2.8	48.1	3.0	[11]
2% Rh/CeO_2[c]	~35	5	2.22	52.1	2.91	[23]
5% Rh/SiO_2	36	4.4	2.28	62.2	3.26	[17]
4% Rh/GNF-H	30	5	2.58	48.3	2.93	This work
5% Rh/GNF-P	30	3.4	2.25	38.1	2.78	This work

[a] ζ: the number of fragments per fragmented molecules [10].
[b] 463 K.
[c] 483 K.

The main reaction (cf. Fig. 5), i.e., ring opening was "selective", meaning that the cleavage of the C–C bonds next to the methyl group was hindered. This type of selectivity is made possible if the surface intermediate of ring opening lies parallel to the catalyst surface (cf. [24], p. 211). The 2MP/nH ratios were relatively high (up to ~10). The "selectivity" of ring opening (mainly the ratio 2MP/nH but also 2MP/3MP) increased at higher H_2 pressures. These conditions favor product desorption rather than further hydrogenolysis of the primary C_6 surface entities (Table 3). Somewhat higher 2MP/nH ratios appeared on Rh/GNF-H. This ratio dropped at higher temperatures (with less surface hydrogen present), reaching ~4 at 513 K at $p(H_2)$ = 120 Torr. As the depth of hydrogenolysis increased (more fragments were produced), the selectivity of 2MP decreased, because of the preferred further hydrogenolysis of the 2MP surface intermediate. Fig. 6 shows plots found rather informative earlier [11,17,22] to summarize the selectivities at several temperatures and H_2 pressures. The selectivities of 3MP, nH and Σ(2MP + $<C_6$) were almost independent in the whole range of parameters. If one separates, however, 2MP from the fragments, the 2MP selectivity increased at higher $p(H_2)$ at each temperature and on both catalysts. Fragmentation consumed mainly 2MP, decreasing its amount. This statement was strictly valid for Rh/GNF-P but the results on Rh/GNF-H indicate an additional hydrogenolysis of the 3MP primary product, at lower hydrogen pressures, and at 498 and 513 K. Both catalysts were insensitive of the reaction conditions as far as the position of the first C–C bond breaking to methylpentanes (in favored positions, farther from the methyl substituent) is concerned. Table 3 shows that the ratio 2MP/3MP is close to 2

Table 3
Ring opening product distribution of two Rh/GNF catalysts (T = 468 K)

$p(H_2)$ (Torr)	Catalyst			
	4% Rh/GNF-H		5% Rh/GNF-P	
	2MP/nH	2MP/3MP	2MP/nH	2MP/3MP
120	6.4	1.4	5.6	1.39
240	7.5	1.53	6.8	1.63
360	8.5	1.7	7.3	1.81
480	10.2	1.73	7.8	1.98

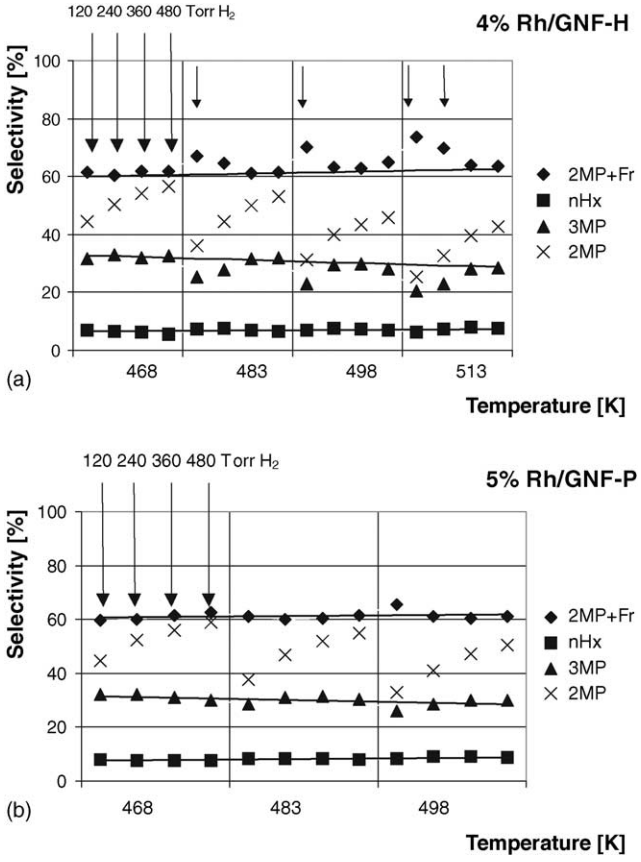

Fig. 6. Selectivity comparison for hexane, 2- and 3-methylpentane and Σ(2MP + fragments) at different temperatures. Four hydrogen pressures are shown at each temperature (denoted by arrows at the lowest temperature. (a) Rh/GNF-H. Small arrows indicate cases where $\Sigma(2MP + <C_6)$ values are higher, thus deviate from the general trend. (b) Rh/GNF-P. The general selectivity trend is valid throughout.

(i.e., random ring opening far from the $–CH_3$ group) on Rh/GNF-P and at highest $p(H_2)$ only. The two types of behavior (if 3MP undergoes also fragmentation or not) represent a principal difference between various Rh catalysts, due to the *actual* surface H concentration on Rh sites, highest, likely on Rh/GNF-P.

4. Conclusions

Rh/GNF catalysts contained well-discernible nanometer-size, rather regular Rh particles on the surface of the GNF support. Rh was partly oxidized during storage in air but was easily reduced with H_2 under reaction conditions. Both catalysts produced mostly methylpentanes with a strong positive hydrogen order. ‘‘Selective’’ ring opening of MCP (to methylpentanes) was observed, indicating a less dissociated, ‘‘flat-lying’’ intermediate. Of the two Rh/GNF samples, Rh/GNF-H exhibited somewhat stronger hydrogenolysis activity, fragment formation being more marked at higher T and lower $p(H_2)$. 2MP was the primary precursor of $<C_6$ products [23]. The nondegradative activity of both Rh/GNF samples was larger than oxide supported Rh catalysts. Due to the pronounced inherent ability of Rh to split C–C bonds [9], Rh/GNF catalysts were not so different from other supported Rh samples as Pt/GNF from conventional Pt catalysts [3,4].

Acknowledgements

We thank Dr. Á. Mastalir (University of Szeged) for preparing the 4% GNF-H sample. Financial support of the Hungarian National Science Foundation (OTKA Grant 37241) and the Fritz-Haber-Institut der MPG (Berlin) is gratefully acknowledged.

References

[1] N.M. Rodriguez, M.-S. Kim, R.T.K. Baker, J. Phys. Chem. B 98 (1994) 13108.
[2] C. Park, R.T.K. Baker, J. Phys. Chem. B 103 (1999) 2453.
[3] R.T.K. Baker, K. Laubernds, A. Wootsch, Z. Paál, J. Catal. 193 (2000) 165.
[4] R.T.K. Baker, N.M. Rodriguez, Á. Mastalir, U. Wild, R. Schlögl, Z. Paál, J. Phys. Chem. B 108 (2004) 14348.
[5] R. Gao, C.D. Tan, R.T.K. Baker, Catal. Today 66 (2001) 19.
[6] T.G. Ros, D.E. Keller, A.J. van Dillen, J.W. Geus, D.C. Koningsberger, J. Catal. 211 (2002) 85.
[7] F.G. Gault, Adv. Catal. 30 (1981) 1.
[8] Z. Paál, in: I.T. Horváth (Ed.), Encyclopedia of Catalysis, 6, Wiley, Hoboken, 2003, p. 116.
[9] U. Wild, D. Teschner, R. Schlögl, Z. Paál, Catal. Lett. 67 (2000) 93.
[10] Z. Paál, P. Tétényi, Nature 267 (1977) 234.
[11] D. Teschner, K. Matusek, Z. Paál, J. Catal. 192 (2000) 335.
[12] F. Garin, G. Maire, Acc. Chem. Res. 20 (1989) 100.
[13] N.M. Rodriguez, A. Chambers, R.T.K. Baker, Langmuir 11 (1995) 3862.
[14] Z. Paál, A. Wootsch, Catal. Today 66 (2001) 12.
[15] D. Briggs, M.P. Seah (Eds.), Practical Surface Analysis, 1, Wiley, Chichester, 1990, , p. 635Appendix 6.
[16] B. Veisz, Z. Király, L. Tóth, B. Pécz, Chem. Mater. 14 (2002) 2882.
[17] D. Teschner, Z. Paál, D. Duprez, Catal. Today 65 (2001) 185.
[18] W.H. Lee, J.G. Lee, P.J. Reucroft, Appl. Surf. Sci. 171 (2000) 136.
[19] R. Schlögl, in: G. Ertl, H. Knözinger, J. Weitkamp (Eds.), Handbook of Heterogeneous Catalysis, 1, VCH-Wiley, Weinheim, 1997, p. 138.
[20] C. Kozlowski, P.M.A. Sherwood, J. Chem. Soc., Faraday Trans. 81 (1985) 2745.
[21] S. Akhter, X.-L. Zhou, J.M. White, Appl. Surf. Sci. 37 (1989) 201.
[22] D. Teschner, L. Pirault-Roy, D. Naud, M. Guérin, Z. Paál, Appl. Catal. A 252 (2003) 421.
[23] D. Teschner, A. Wootsch, T. Röder, K. Matusek, Z. Paál, Solid State Ionics 141/142 (2001) 709.
[24] D. Teschner, Z. Paál, D. Duprez, J. Mol. Catal. 179 (2002) 201.